

Superparamagnetism and transport properties of ultrafine $\text{La}_{2/3}\text{Ca}_{1/3}\text{MnO}_3$ powders

Run-Wei Li^{1,3}, Han Xiong², Ji-Rong Sun¹, Qing-An Li¹,
Zhi-Hong Wang¹, Jian Zhang¹ and Bao-Gen Shen¹

¹ State Key Laboratory of Magnetism, Institute of Physics and Centre for Condensed Matter Physics, Chinese Academy of Sciences, PO Box 603, Beijing 100080, China

² State Key Laboratory of Superconductors, Institute of Physics and Centre for Condensed Matter Physics, Chinese Academy of Sciences, PO Box 603, Beijing 100080, China

E-mail: rwli@g203.iphy.ac.cn (Run-Wei Li)

Received 4 August 2000, in final form 15 November 2000

Abstract

Magnetic and transport properties of ultrafine $\text{La}_{2/3}\text{Ca}_{1/3}\text{MnO}_3$ (LCMO) powders synthesized by mechanical alloying with a grain size of about 18 nm have been investigated. It is found that the powder sample is superparamagnetic above 95 K. The blocking temperature (T_B) obtained from the characteristic peak in the zero-field-cooled magnetization decreases with the measuring applied field, and can be well fitted by $T_B = a \ln(\mu_0 H) - b$. The spontaneous magnetization of the powder sample is only 38% of that in the corresponding bulk LCMO. Unlike conventional bulk LCMO, the powder compact is insulating from 5 K to 300 K. The low-temperature magnetoresistance (MR), defined as $\text{MR} = \Delta R/R(0)$ ($R(0)$ being the zero-field resistance), is approximately 100% under a field of 6 T, much higher than that of the conventional bulk LCMO (50–60%). When the temperature is above T_B , the low-field MR associated with the spin-polarized tunnelling between grains cannot be observed; however, the high-field MR increases linearly with the applied field. The small grain size and the surface layer in which many oxygen vacancies and defects induced by high-energy milling exist are suggested to be responsible for the present observations.

1. Introduction

The magnetic and transport properties of rare-earth manganites of formula $\text{Ln}_{1-x}\text{A}_x\text{MnO}_3$ (Ln = rare earth, A = Ca, Sr, Ba, Pb) have been systematically investigated, for single crystals, thin films, and polycrystalline samples, due to their importance for fundamental research and potential applications [1–5]. Most attention has been focused on the prototypical compound with x near 0.33, which exhibits an optimal ferromagnetism and magnetoresistance.

³ Author to whom any correspondence should be addressed. Fax: (86)-10-82649485; telephone: 010-82649251.

It was found that the prototype compound, such as $\text{La}_{2/3}\text{Ca}_{1/3}\text{MnO}_3$, shows a metal–insulator transition with a peak in the resistance and magnetoresistance near the Curie temperature (T_C). A large negative magnetoresistance (MR) at low magnetic fields was also observed in the polycrystalline sample, which was attributed to the spin-polarized tunnelling between grains [6]. Very recently, attention has been drawn towards nanocrystalline perovskite manganites. Mahesh *et al* [7] investigated the effects of particle size on the electron transport and magnetic properties of $\text{La}_{0.7}\text{Ca}_{0.3}\text{MnO}_3$ and found that the T_C and metal–insulator transition temperature (T_P) decrease with the particle size. Spin-glass behaviours have been observed in ultrafine $\text{La}_{0.5}\text{Sr}_{0.5}\text{MnO}_3$ [8] and $\text{La}_{0.7}\text{Ca}_{0.3}\text{MnO}_3$ [9]. Ziese [10] and Balcells *et al* [11] emphasized the interface effects on transport properties in $\text{La}_{0.7}\text{Ca}_{0.3}\text{MnO}_3$ film and $\text{La}_{2/3}\text{Sr}_{1/3}\text{MnO}_3$ nanoscale powders, respectively, and showed that the tunnelling barrier is a noncollinear ferromagnet. However, in order to shed some light on the applications of the nanocrystalline perovskite manganites, more detailed investigation is still inquired. In this paper, additional information regarding the magnetic and electrical properties of nanoscale $\text{La}_{2/3}\text{Ca}_{1/3}\text{MnO}_3$ powders synthesized by high-energy ball milling have been presented. We found that, very much unlike the conventional bulk LCMO, the powder sample is superparamagnetic above 95 K and behaves as an insulator between 5 K and 300 K; a large low-temperature MR was observed under a field of 6 T.

2. Experiment

A polycrystalline sample of $\text{La}_{2/3}\text{Ca}_{1/3}\text{MnO}_3$ (LCMO) was prepared by the conventional ceramic route. A well-mixed stoichiometric mixture of La_2O_3 , CaCO_3 , MnCO_3 was calcined at 800 °C in air for 24 h. Then the resulting powders were reground, pressed into pellets, and sintered at 1300 °C for 48 h, then furnace-cooled to room temperature. Ultrafine LCMO powders were prepared through grinding the as-obtained bulk LCMO by high-energy ball milling. In order to measure the resistance of the ultrafine powders, the powder compact was made under a high pressure of 6 GPa at room temperature. The phase purity and crystal structure of the synthesized powders were examined by means of powder x-ray diffraction (XRD), performed on a Rigaku x-ray diffractometer with a rotating anode and Cu $K\alpha$ radiation. All of the XRD peaks correspond to a cubic perovskite structure. The crystalline size determined from the XRD peak width by Scherrer's formula is about 18 nm. The Mn^{4+} content was examined by redox titration. The magnetization measurements were performed in a commercial SQUID magnetometer. The resistance was measured by the standard four-probe method with the current parallel to the magnetic field. The MR ratio is defined by $\text{MR} = [R(0) - R(H)]/R(0)$, where $R(0)$ and $R(H)$ are the resistance in the absence and presence of an external field, respectively.

3. Results and discussion

Figure 1 shows the temperature dependence of the magnetization (M – T) of the ultrafine powders measured by increasing the temperature under a field of 0.02 T in zero-field-cooled (ZFC) and field-cooled (FC) modes, respectively. In the ZFC mode, the magnetization increases at first, then decreases with increasing temperature. The M – T curve measured under a magnetic field of 0.02 T exhibits a peak at 95 K followed by a broadened ferromagnetic-to-paramagnetic transition. A large difference between the ZFC and FC magnetizations below 260 K can be clearly observed, and the ferromagnetic-to-paramagnetic transition is more inconspicuous in the FC mode. The M – T curves measured at various magnetic

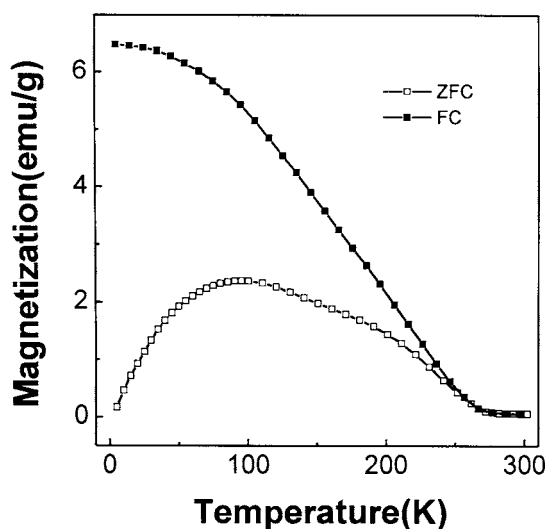


Figure 1. The temperature dependence of the magnetization measured under a magnetic field of 0.02 T in the ZFC and FC modes on heating.

fields in the ZFC mode are shown in figure 2. Under the high measuring magnetic field (higher than 0.05), the M - T curve shows a linear decrease with increasing temperature well above the ZFC magnetization peak temperature, which is consistent with the high-field/low-temperature approximation of the Langevin function. The above features are characteristic of superparamagnetic behaviours. The peak temperature of the ZFC M - T curve, defined as the blocking temperature, decreases with increasing magnetic field as shown in the inset of figure 2. It was found that, in the granular Co-Ag samples, the initial decrease of T_B with applied magnetic field is quadratic [12]. However, the T_B of our powder sample can be fitted very well by $T_B = a \ln(\mu_0 H) - b$, where $a = 12.5$ and $b = 17$ K. This unconventional magnetic field dependence of the T_B may be related to the interparticle interaction [14–16], which needs further investigation.

Measurements on the demagnetization processes, which are defined here as magnetization processes with a field of 5 T decreasing to -0.01 T, were made at various temperatures and the results are shown in figure 3. With increasing temperature, the remanence and coercivity decrease and become zero above 250 K. When temperature is above T_B , an anomaly in the remanence can be seen and becomes more obvious with increasing temperature. The phenomenon can be explained well by taking into account the distribution of particle sizes. As we know, for a system consisting of magnetic particles with finite volume, T_B has a relation to the particle volume (V), which can be described as $T_B \propto V$ [17]. As a result, the distribution of particle sizes causes a distribution of the T_B . For example, when the temperature is 140 K, particles whose sizes are small and for which $T_B < 140$ K are superparamagnetic and exhibit zero coercivity and remanence; however, large particles for which T_B is higher than 140 K are still ferromagnetic at that temperature. Consequently, the coexistence of ferromagnetic particles and superparamagnetic ones brings about the anomaly in the remanence.

In figure 4, the magnetization as a function of the applied field (M - H) at various temperatures is plotted. The ultrafine powders exhibit ferromagnetic characteristics at low magnetic field below 250 K. As the temperature decreases, the M - H curve bends more, but no sign of saturation is present. The absolute value of the magnetization at 5 K under 5 T

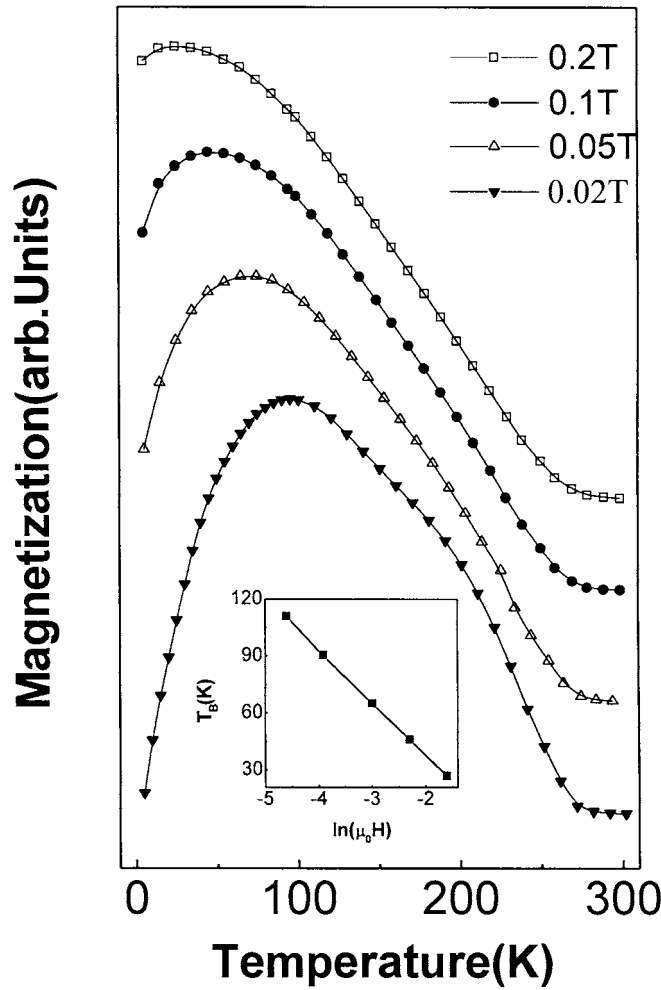


Figure 2. The temperature dependence of the magnetization under various magnetic fields in the ZFC mode. The inset shows T_B as a function of the measuring magnetic field.

is much smaller than the value expected from the Mn^{3+}/Mn^{4+} ratio, and is only 38% of that for the conventional bulk LCMO. The lower saturation magnetization can be attributed to the presence of noncollinear interface layers between grains. A lower limit of the layer thickness (t) can be estimated assuming that the noncollinear interface layers have zero magnetization. With this assumption, the layer thickness can be expressed as

$$t = (r/2)\{1 - [M_s/M_{s0}]^{1/3}\}$$

where M_s and M_{s0} represent the saturation magnetization of the ultrafine powders and the conventional bulk sample, respectively. Rough estimation indicates that interface layers 1.4 nm thick for the $r = 18$ nm powder sample can reduce the saturation magnetization as described above.

In order to study the transport properties of the ultrafine powder compact, the temperature dependences of the resistance ($R-T$) and magnetoresistance ($MR-T$) were measured and they are shown in figure 5. For comparison, the $R-T$ and $MR-T$ curves of the corresponding bulk

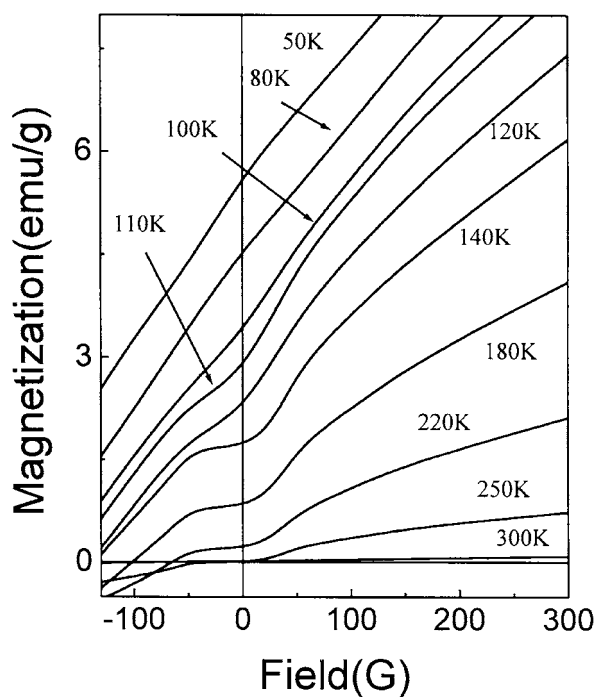


Figure 3. The demagnetization of the ultrafine LCMO powders measured after a field of 5 T was applied at various temperatures.

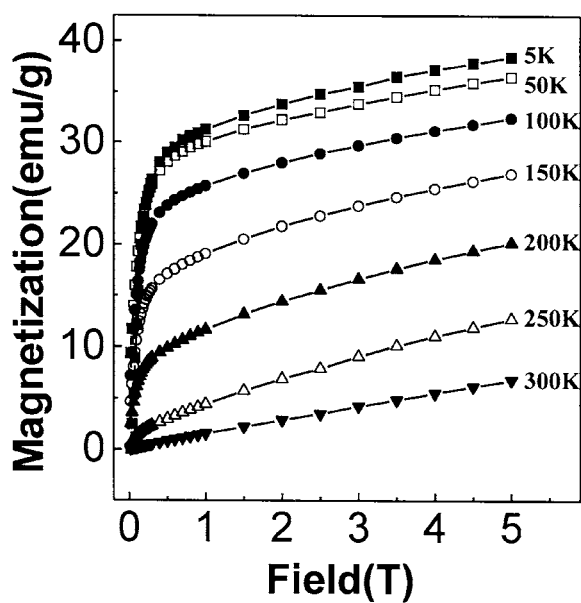


Figure 4. The magnetization of the ultrafine LCMO powders as a function of the magnetic field at various temperatures.

LCMO are also plotted in figure 5 as the dashed lines. The resistance of the powder compact is several orders of magnitude larger than that of the bulk LCMO and it is insulating from 5 to 300 K. The metal-insulator transition could not be observed, though a magnetic field of 6 T was applied. When the temperature is below 30 K, an obvious upturn in the $R-T$ curve appears, and this can be ascribed to the Coulomb blockade contribution to the resistance, as reported

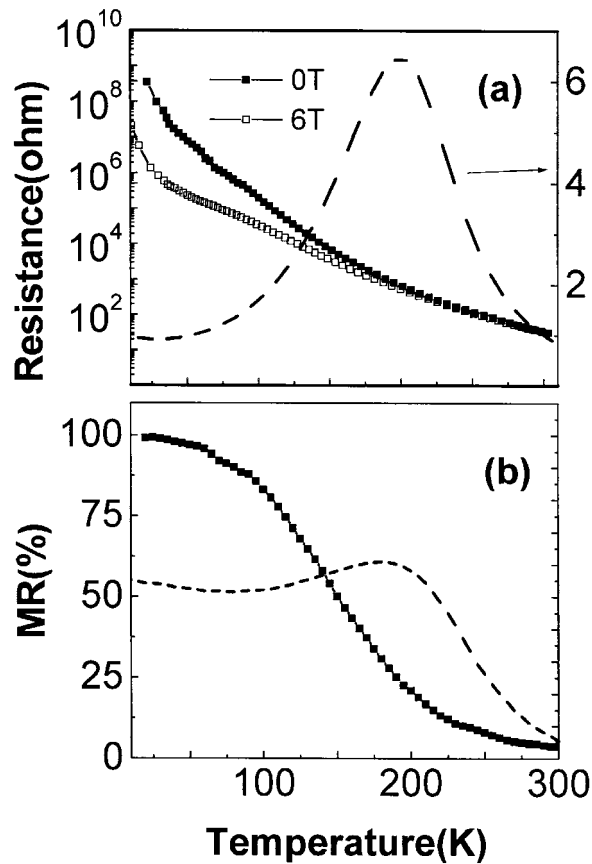


Figure 5. (a) The temperature dependence of the resistance measured under magnetic fields of 0 T and 6 T, respectively. (b) The temperature dependence of the MR under a field of 6 T—the symbol line for the powder compact and the dashed line for the conventional bulk LCMO.

by Balcells *et al* [11] and Coey *et al* [13]. The MR ratio of the powder compact is higher below 150 K and lower above 150 K than that of its parent bulk LCMO. It is notable that the MR ratio increases monotonically with decreasing temperature and approaches a maximum of 100% at 5 K. The field-dependent resistance $R(H)$ (normalized by the zero-field value) and magnetization (normalized by the 5 T value) at 100 K are shown in figure 6. Interestingly, the sharp drop in resistance at low field, which is related to the spin-polarized tunnelling between grains, is indistinct. However, the MR (at 100 K) increases linearly with the magnetic field without signs of saturation up to 5 T. A striking feature of the powder compact is that, above 0.1 T, the MR sensitivity $S = \delta(\text{MR})/\delta H$ remains nearly constant at -0.08 (see the inset of figure 6)—much higher than that of the conventional bulk $\text{La}_{2/3}\text{Sr}_{1/3}\text{MnO}_3$ (-0.03) reported by Hwang *et al* [6].

To explain the transport properties described above, the interface layers between grains have to be considered. In the milling process, many defects were inevitably produced in the interface layers due to the intrinsic characteristics of ball milling. Moreover, the redox titration results show that the Mn average valence of the ultrafine powders decreases from 3.328 for the bulk LCMO to 3.26. In other words, a lot of oxygen vacancies exist, probably in the interfaces. Oxygen vacancies break parts of the $\text{Mn}^{3+}-\text{O}^{2-}-\text{Mn}^{4+}$ networks and introduce forbidden paths

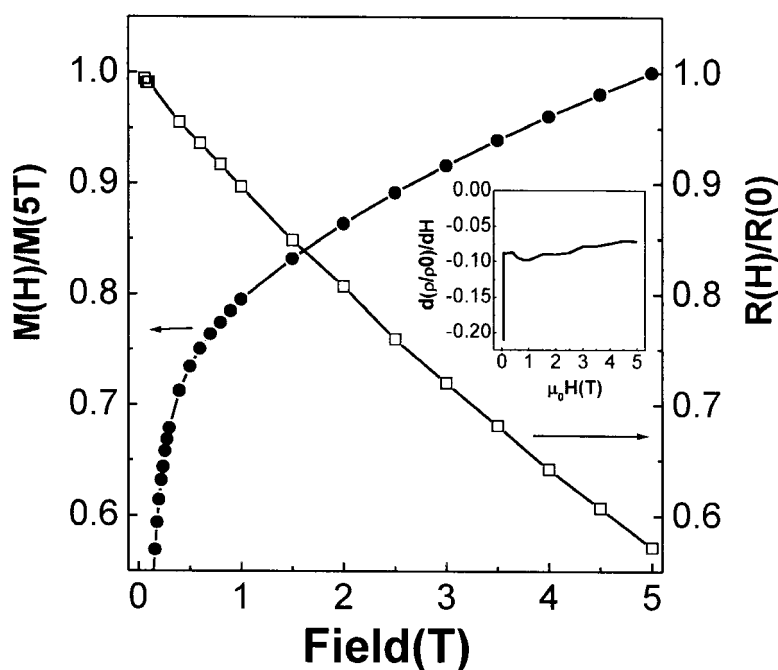


Figure 6. The field-dependent resistance $R(H)$ normalized by the zero-field value and magnetization normalized by the 5 T value at 100 K. The inset shows the MR sensitivity as a function of the magnetic field.

for conductance electrons. A more important role of the vacancies is the electron localization through the Coulomb interaction. The oxygen vacancies have the effective charge of $+2e$, which is favourable for electron localization. As a result, the double-exchange interaction is weakened due to the existence of defects and oxygen vacancies. The other factor affecting the electron mobility is the larger surface area associated with the small grain size. The energy level of the Mn ions at the surface is different from that deep inside the bulk. Thus, e_g electrons near the surface are likely to be localized even without defects and oxygen vacancies. In general, the interfaces between grains are insulating. In other words, a sample with small grain size and large number of boundaries is of a ferromagnetic/insulating/ferromagnetic tunnelling junction structure. Therefore, the sample behaves as an insulator in the temperature range from 5 to 300 K.

When temperature is higher than T_B , the grain magnetization orients randomly, which strongly suppresses the intergrain spin-polarized tunnelling process and can explain well the disappearance of the steep decrease of the resistance at low magnetic fields. From the above discussion, we can draw the conclusion that a nanostructure material or device based on intergrain spin-polarized tunnelling should be operated at a temperature below T_B .

Acknowledgments

We acknowledge T S Ning and S Y Fan for their help with the measurement. This work was supported by the National Natural Science Foundation of China and the State Key Programme of Basic Research of China.

References

- [1] Urushihara A, Moritomo Y, Arima T, Asamitsu A, Kido G and Tokura Y 1995 *Phys. Rev. B* **51** 14 103
- [2] Hwang H W, Cheong S-W, Radaelli P G, Marezio M and Batlogg B 1995 *Phys. Rev. Lett.* **75** 914
- [3] van Helmolt R, Wecker J, Holzapfel B, Schultz L and Samwer K 1995 *Phys. Rev. Lett.* **71** 2331
- [4] Sun J R, Yeung C F, Zhao K, Zhou L Z, Leung C H, Wong H K and Shen B G 2000 *Appl. Phys. Lett.* **76** 1164
- [5] Li R W, Wang Zhi-hong, Chen Xin, Sun Ji-rong, Shen Bao-gen and Yan Chun-hua 2000 *J. Appl. Phys.* **87** 5597
- [6] Hwang H Y, Cheong S-W, Ong N P and Batlogg B 1996 *Phys. Rev. Lett.* **77** 2041
- [7] Mahesh R, Mahendiran R, Raychaudhuri A K and Rao C N R 1996 *Appl. Phys. Lett.* **68** 2291
- [8] Wang Z H, Ji T H, Wang Y Q, Chen X, Li R W, Cai J W, Sun J R, Shen B G and Yan C H 2000 *J. Appl. Phys.* **87** 5582
- [9] Muroi M, Street R and McCormick P G 2000 *J. Appl. Phys.* **87** 5579
- [10] Ziese M 1999 *Phys. Rev. B* **60** R738
- [11] Balcells L, Fontcuberta J, Martínez B and Obradors C 1998 *Phys. Rev. B* **58** R14 697
- [12] Zhang Y D, Budnick J I, Hines W A, Chien C L and Xiao J Q 1998 *Appl. Phys. Lett.* **72** 2053
- [13] Coey J M, Berkowitz A E, Balcells L, Putris F F and Barry A 1998 *Phys. Rev. Lett.* **80** 3815
- [14] Chantrell R W, Walmsley N S, Gore J and Maylin M 1999 *J. Appl. Phys.* **85** 4340
- [15] Dormann J L, D'Orezio F, Lucari F, Tronc E, Prene P, Jolivet J P, Fiorani D, Cherkaoui R and Nogues M 1996 *Phys. Rev. B* **53** 14 291
- [16] Dai J B, Wang J Q, Sangregoric C, Fang J Y, Carpenter E and Tang J K 2000 *J. Appl. Phys.* **87** 7397
- [17] Néel L 1949 *Ann. Geophys. (CNRS)* **5** 99